Magnetic Moment of the Proton in Units of the Nuclear Magneton*

H. S. Boyne† and P. A. Franken‡
The University of Michigan, Ann Arbor, Michigan
(Received February 3, 1961)

A new method for measuring the magnetic moment of the proton in units of the nuclear magneton is described. The method differs from the work of others in that the cyclotron frequency of free low-energy H_2^+ ions is measured with a low-power absorption technique as a function of magnetic field. The extrapolation technique of Franken and Liebes is utilized to correct for shifts produced by electrostatic fields. The measurements yield $\mu_p(H_2O)/\mu_n = 2.792\,83 \pm 0.000\,06$. This determination is approximately 50 ppm higher than the results of other workers.

INTRODUCTION

In this paper we wish to describe a new method for measuring the magnetic moment of the proton in units of the nuclear magneton and discuss our preliminary determination. Our value is in marked disagreement with the results obtained by other workers.[1–3]

The determination of this quantity is achieved by measuring the ratio of the proton nuclear spin resonance frequency $\omega_p = 2\mu_p H/\hbar$ and the proton cyclotron frequency $\omega_c = eH/Mc$ in the same magnetic field H. This ratio yields the magnetic moment of the proton μ_p, in units of the nuclear magneton, $\mu_n = e\hbar/2Mc$.

The primary experimental difficulties arise from the determination of the cyclotron resonance frequency. The observed resonance absorption is subject to significant electrostatic shifts due to the presence of inhomogeneous electrostatic fields, produced by space charge and applied trapping potentials.

In the research of other workers,[1–3] various forms of miniature cyclotrons were constructed and operated in either accelerating or decelerating modes. The ion currents were collected and studied as a function of frequency. Because of the dynamics of the acceleration processes and the presence of average radial electric fields, the observed current maxima occurred at frequencies shifted from the value eH/Mc by small but not negligible amounts. These shifts had to be accounted for in the determination of μ_p/μ_n.

In the experiment described here, the cyclotron resonance absorption of a spatially small cloud of thermal ions is measured with a low-power technique developed by Franken and Rogers.[4] The observed resonance frequency exhibits electrostatic shifts as large as several hundred parts per million (ppm). These shifts are evaluated with the magnetic field extrapolation technique developed by Franken and Liebes[5,6] for the problem of electron cyclotron resonance absorption and the determination of the proton moment in units of the Bohr magnetron.

In the present experiment the measurements were performed in the range of 8000 to 12 500 gauss. In the work currently being undertaken, and to be described in a later paper, the apparatus has been modified to permit measurements up to 20 000 gauss with an anticipated several fold increase in accuracy.

A. DESCRIPTION OF THE EXPERIMENT

The cyclotron resonance is measured in a dilute cm-sized cloud of thermal energy ions that are generated by electron impact ionization. The resonance is detected by applying a weak rf electric field to the cloud. This electric field is oriented at right angles to the uniform magnetic field and is produced by a marginal oscillator sensitive to small power losses. When the frequency of the electric field is set at the cyclotron frequency, the ions absorb a small amount of power which is detected as a diminution in the output of the oscillator. (This is simply an electric analog to nuclear magnetic resonance absorption methods.) An important feature of this technique is that the ion cloud is not significantly disturbed by the power absorption.

Hydrogen molecular ions (H_2^+) are utilized instead of protons (H^+) for the cyclotron resonance because the cross section for their production is $\sim$50 times larger. The conversion of the resonance data on H_2^+ to H^+ requires only the very accurately known mass ratio

* This research was supported in part by the Atomic Energy Commission and is based in part on a dissertation submitted by one of us (H. S. Boyne) in partial fulfillment of the requirements for the degree of Doctor of Philosophy in Physics at The University of Michigan.

† Present address: National Bureau of Standards, Washington 25, D. C.

‡ Alfred P. Sloan Foundation Fellow.

[1] J. A. Hipple, H. Sommer, and H. A. Thomas, Phys. Rev. **76**, 1877 (1949); H. Sommer, H. A. Thomas, and J. A. Hipple, *ibid.* **81**, 697 (1950).

[2] F. Bloch and C. D. Jeffries, Phys. Rev. **80**, 305 (1950); C. D. Jeffries, *ibid.* **81**, 1040 (1951); K. R. Trigger, Bull. Am. Phys. Soc. **3**, 220 (1956).

[3] D. J. Collington, A. N. Dellis, J. H. Sanders, and K. C. Turberfield, Phys. Rev. **99**, 1622 (1956). The value of μ_p/μ_n quoted in our work is from K. C. Turberfield, J. H. Sanders, and A. N. Dellis (to be published). We wish to thank Dr. Sanders for his communication of this result.

[4] This work was undertaken at Stanford University with the support of the Office of Naval Research and the Research Corporation. Brief accounts are given in the Office of Naval Research progress reports of 1955 and 1956. This method is closely related to the relatively high power absorption techniques reported by H. Sommer and H. A. Thomas, Phys. Rev. **78**, 806 (1950), and H. J. Woodruff and J. H. Gardner, Rev. Sci. Instr. **27**, 378 (1956).

[5] P. A. Franken and S. Liebes, Jr., Phys. Rev. **104**, 1197 (1956).

[6] S. Liebes, Jr., Ph.D. thesis, Stanford University, 1957 (unpublished); S. Liebes, Jr., and P. A. Franken, Phys. Rev. **116**, 633 (1959).

$M_{H^+}/M_{H_2^+}$. The cyclotron frequency of H_2^+ is $\sim$7.5 Mc/sec in a field of 10 000 gauss.

It is experimentally more convenient to measure the nuclear magnetic resonance frequency of deuterons ω_d instead of protons ω_p. In a magnetic field of 10 000 gauss ω_d is $\sim$6.5 Mc/sec as compared with 42.5 Mc/sec for ω_p. Since the deuteron and the (H_2^+) resonance frequencies are of the same magnitude, they can be measured with common apparatus. This is particularly convenient because the extrapolation procedure to be described requires reasonably rapid measurements of the frequency ratio at different magnetic fields. The measured ratio $\omega_d/\omega_c(H_2^+)$ is readily converted to the desired quantity $\omega_p/\omega_c(H^+)$:

$$\frac{\omega_d}{\omega_c(H_2^+)}\frac{\omega_p}{\omega_d}\frac{M_{H^+}}{M_{H_2^+}}=\frac{\omega_p}{\omega_c(H^+)}=\frac{\mu_p}{\mu_n},$$

where ω_p/ω_d is the very accurately measured ratio of the proton and deuteron spin resonance frequencies.

In order to correct for the electrostatic shifts in the cyclotron frequency three assumptions are made which are subject to experimental verification: (1) the ion orbit radii are small compared to distances in which the electrostatic field varies appreciably; (2) the electrostatic shift is small; and (3) the electrostatic field is independent of the magnetic field in a chosen range of magnetic field variation.

When assumptions (1) and (2) obtain, it can be shown[6,7] that the experimentally observed frequency ratio ω_c'/ω_d is related to the desired quantity ω_c/ω_d by the expression

$$\frac{\omega_c'}{\omega_d}=\frac{\omega_c}{\omega_d}\left[1-\frac{K}{H^2}\right],$$

where H is the magnetic field and K is a function only of the electrostatic field distribution. This expression suggests the measurement of ω_c'/ω_d as a function of magnetic field. If assumption (3) is satisfied, a linear dependence of ω_c'/ω_d with respect to $1/H^2$ should be observed. Thus a linear extrapolation to $1/H^2=0$ would determine ω_c/ω_d.

The ratio ω_c'/ω_d has been studied as a function of $1/H^2$ for magnetic fields ranging from 8000 to 12 500 gauss and for widely varied electrostatic conditions. For each run, five to nine points were taken in this magnetic field interval. Analysis of all the data indicates that any systematic deviations from a straight line dependence are less than 1.5 ppm in this interval.

B. ION CYCLOTRON RESONANCE

We wish to study the power absorbed by a cloud of ions situated in a uniform magnetic field H and subjected to a homogeneous radio-frequency electric field orthogonal to H. It will be useful to review some of the conditions of this experiment in order to establish the magnitudes of relevant physical quantities.

The cyclotron tube is initially evacuated to a pressure of $\sim 2\times10^{-8}$ mm Hg and the components are kept clean by repeated induction heating. Hydrogen molecular gas is allowed into the chamber by a control leak so that an operating pressure in the range of 5×10^{-7} to 10^{-5} mm Hg can be maintained. Ions are created by electron bombardment with 40- to 90-v electrons in a beam current not greater than 10^{-6} amp. The cross section for the ionization process is $\sim10^{-16}$ cm^2 and the mean lifetime of an ion is typically $\sim10^{-4}$ sec. This leads to a steady state of $\sim10^4$ ions in the chamber. A steady state of $\sim10^4$ electrons is maintained in the chamber because of the electron ionizing beam. The ionization process contributes negligible kinetic energy to the molecular ions (momentum conservation) and the oscillating electric field is maintained at $\sim10^{-3}$ volt/cm so that the mean energy absorbed by an ion at resonance is $\sim$0.05 ev [see Eq. (1) below].

If a uniform rf electric field of amplitude E_0 and frequency ω is applied transverse to a constant homogeneous magnetic field H, the power absorbed by the ion cloud as a function of ω is[6,7]

$$P(\omega)=\frac{N(eE_0)^2}{2M}\int_0^\infty\frac{\sin^2[\frac{1}{2}(\omega-\omega_c)t]}{(\omega-\omega_c)^2}L(t)dt, \quad (1)$$

where N is the number of ions created per second, e and M are the ionic charge and mass, $\omega_c=eH/Mc$ is the ion cyclotron frequency, and $L(t)$ is a normalized distribution function such that $L(t)dt$ is that fraction of N having lifetimes between t and $t+dt$ seconds.

In the analysis leading to Eq. (1) it is assumed that the percentage linewidth of the observed resonance is small, which assumption accounts for the absence of an antiresonant term as well as perturbation terms due to a component of rf electric field collinear with H.[6] The corrections required for linewidths observed in this experiment are completely negligible compared with 1 ppm.

There are two very important implications of Eq. (1):

(1) The observed power absorption is symmetric in the quantity $(\omega-\omega_c)$, *regardless of the lifetime distribution function* $L(t)$.

(2) There is no explicit dependence of the power absorption on the initial velocity distribution of the ions. [The velocity distribution does play a role, of course, in the determination of $L(t)$.]

C. LIFETIME CONSIDERATIONS AND LINE SHAPE

Experimental studies of the cyclotron resonance indicate that there are two major contributions to the line shape. One is due to the inhomogeneous electric field present in the cyclotron resonance chamber and is discussed in Secs. D and E. The other contribution is due to the finite lifetimes of the ions in the resonance

[7] H. S. Boyne, Ph.D. thesis, University of Michigan, Ann Arbor, Michigan, 1959 (unpublished).

chamber and has no effect on the line-shape symmetry. [See Eq. (1).]

The factors which influence the lifetimes are so involved that no detailed treatment is attempted. Nevertheless, it is interesting to note that the use of a lifetime distribution function $L(t)$ derived from admittedly crude models of the lifetime-controlling mechanisms does approximate the features of the experimentally observed line shapes. Owing to the high vacuum, the major lifetime-controlling mechanism is the time of flight of the ion from some point in the resonance chamber to the walls of the chamber which are perpendicular to the applied magnetic field. That is, the time it takes the ion to be swept out of the chamber in a direction parallel to the applied magnetic field. If an electrostatic trapping field is applied in this direction the linewidth decreases markedly, indicating that the lifetime of the ion is increased.

We now consider three idealized models. The z direction of a right-hand Cartesian coordinate system is situated collinear with the applied magnetic field and the length of the resonance chamber in the z direction is l. The electron beam which ionizes the hydrogen molecule is collinear with the magnetic field and it is assumed that within the resonance chamber the probability that an ion is created in any element dz of the chamber is independent of z. It is further assumed that the electrostatic field is constant along the z axis so that an ion created at rest in the chamber undergoes a uniform acceleration in the z direction. Therefore, $z=\frac{1}{2}at^2$, and the probability that an ion created in any element dz lives between t and $t+dt$ seconds before striking the wall of the chamber is

$$L(t)dt=dz/l=atdt/l.$$

Therefore,

$$\begin{aligned} L(t)&=at/l, \quad 0\leqslant t\leqslant (2l/a)^{\frac{1}{2}} \\ &=0, \quad t>(2l/a)^{\frac{1}{2}}. \end{aligned} \tag{2}$$

Substitution of $L(t)$ into Eq. (1) yields a resonance line shape

$$P(\omega-\omega_c)=\frac{ct_x^2}{x^4}[1-\cos x-x\sin x+\tfrac{1}{2}x^2], \tag{3}$$

where

$$t_x=(2l/a)^{\frac{1}{2}}; \quad x=t_x(\omega-\omega_c); \quad c=\text{const.}$$

The derivative of Eq. (3) is

$$P'(\omega-\omega_c)=-\frac{ct_x^2}{x^5}\times[4(1-\cos x)+x^2(1+\cos x)-4x\sin x]. \tag{4}$$

This derivative is compared with an experimental curve in Fig. 1. It should be noted that the comparison of derivatives usually provides a more sensitive test of agreement than does a comparison of the line shapes themselves.

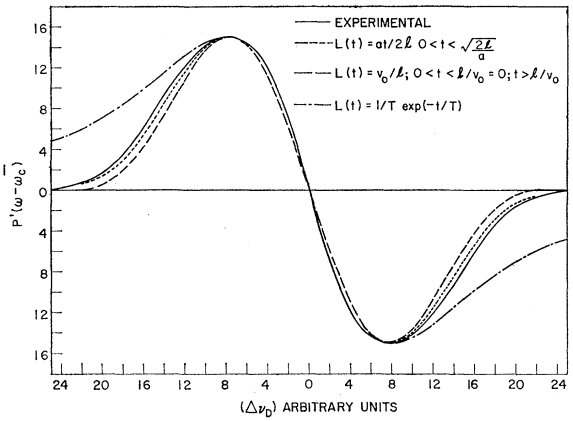

FIG. 1. Plot of experimental and theoretical line shapes.

A second model for the lifetime controlling mechanism assumes there is no electric field in the z direction of the chamber and that all ions are created with a z component of velocity v_0. Therefore, $z=v_0t$ and the probability that an ion created in an element dz will live between t and $t+dt$ seconds is

$$L(t)dt=dz/l=(v_0/l)dt.$$

Therefore,

$$\begin{aligned} L(t)&=v_0/l, \quad 0\leqslant t\leqslant l/v_0 \\ &=0, \quad t>l/v_0. \end{aligned} \tag{5}$$

Substitution of $L(t)$ into Eq. (1) yields

$$P(\omega-\omega_c)=\frac{ct_x^2}{x^2}\left[1-\frac{\sin x}{x}\right], \tag{6}$$

with a derivative

$$P'(\omega-\omega_c)=-\frac{ct_x^2}{x^3}\left[2+\cos x-\frac{3\sin x}{x}\right], \tag{7}$$

where

$$t_x=l/v_0; \quad x=t_x(\omega-\omega_c); \quad c=\text{const.}$$

This derivative is compared with the experimental curve in Fig. 1.

A third model can be readily developed which, because of the disagreement with experiment, confirms that the background gas is unimportant. This model assumes that the lifetime controlling mechanism is due to gas collisions. The lifetime distribution function then becomes

$$L(t)=(1/T)e^{-t/T}, \tag{8}$$

where T is the mean time between gas collisions. Equation (8) yields the Lorentz line shape

$$P(\omega-\omega_c)=\tfrac{1}{2}cT^2/(1+x^2), \tag{9}$$

with a derivative

$$P'(\omega-\omega_c)=-cT^2x/(1+x^2), \tag{10}$$

where $x=(\omega-\omega_c)T$.

Equations (4), (7), and (10) and an experimental line

shape derivative are plotted in Fig. 1, where the predicted and experimental curves have been normalized at their maxima. The experimental line shape corresponds closely to the wall collision broadened models in contrast to the gas collision model. It would be fallacious to draw important conclusions on the basis of these models as they are so idealized. However, the relatively good agreement suggests that lifetime mechanisms related to these simple forms do play a decisive role in determining $L(t)$.

D. EFFECT OF STATIC ELECTRIC FIELDS

A homogeneous component of static electric field parallel to the magnetic field will accelerate the ions in that direction and a transverse component will cause them to drift in a direction perpendicular to both fields. Thus a static homogeneous electric field alters the ion trajectories, and consequently the lifetime distribution $L(t)$, but it does not produce a shift in the cyclotron resonance frequency, nor does it affect the symmetry of the resonance line.

The effects of an inhomogeneous static electric field arising from space charge as well as applied potentials have been considered by Liebes and Franken.[5,6] They have shown that the observed frequency of maximum power absorption ω' is related to the true cyclotron frequency ω_c by the expression:

$$\omega'=\omega_c\left\{1-\frac{Mc^2}{2eH^2}\left[4\pi\rho_0-\left(\frac{\partial E_z}{\partial z}\right)_0\right]\right\}, \tag{11}$$

where the charge density ρ_0 and $(\partial E_z/\partial z)_0$ are evaluated at the orbit center. The assumptions employed for this derivation are that the frequency shift is small and the ion radii are small compared with distances in which the electric field varies appreciably.

E. EXTRAPOLATION PROCEDURE[8]

For convenience, Eq. (11) is rewritten in the form

$$\omega'=\omega_c\left[1-\frac{Mc^2}{2eH^2}\Gamma\right], \tag{12}$$

where

$$\Gamma=\left[4\pi\rho_0-\left(\frac{\partial E_z}{\partial z}\right)_0\right]=\left[\left(\frac{\partial E_x}{\partial x}\right)_0+\left(\frac{\partial E_y}{\partial y}\right)_0\right].$$

Since the field term Γ is a function of position within the chamber, Eq. (12) expresses the spatial dependence of ω'. Multiplication by $1/\omega_d$ yields

$$\omega'/\omega_d=(\omega_c/\omega_d)\left[1-\frac{Mc^2}{2eH^2}\Gamma\right]. \tag{13}$$

[8] Some of the analysis in this section duplicates material in reference 6 and is included here for completeness.

If Γ is independent of the applied magnetic field, over a specified range, then a plot of ω'/ω_d vs $1/H^2$ in that range will extrapolate linearly to the value ω_c/ω_d at $1/H^2=0$. This extrapolation procedure is basic to the present experiment since it provides the only feasible method of determining ω_c/ω_d from the measured values ω_c'/ω_d. The assumption that Γ is independent of H is subject to experimental verification, as discussed in Sec. N, but it will be examined briefly now in order to obtain some *a priori* justification for its employment.

At $\sim$10 000 gauss, the cyclotron ion radii are $\sim$200 times smaller than the dimensions of the cyclotron resonance chamber. Therefore the decrease in orbit size as the magnetic field is increased should have very little effect on the ion space charge distribution. However, the transverse drift velocity of the ions is sensitive to magnetic field variations and the excursions of the ions caused by this drift must be considered. Typical lifetimes are estimated to be $\simeq 10^{-4}$ sec from independent considerations of linewidths and signal strength. With $\sim 10^4$ ions residing in the chamber, the space charge fields are expected to be less than 1 v/cm. For an average electrostatic field of $\sim 10^{-3}$ esu and $H=10^4$ gauss, the ions will drift a distance of $\sim 10^{-1}$ cm. The geometry of the electrostatic field suggests that this displacement of the orbit center is circular rather than rectilinear. Since the dimensions of the resonance chamber are of the order of 1 cm one might expect that the electric field term Γ should be relatively insensitive to H.

Inspection of Eq. (1) shows that if all ions in the chamber exhibit their maximum power absorption at the same frequency ω', the power absorption curve is symmetric about the frequency $\omega=\omega'$. Such a curve may be represented by the expression

$$P(\omega-\omega')=\psi[\alpha(\omega-\omega')^2], \tag{14}$$

where small values of the linewidth parameter α are associated with broad resonance lines. In general, however, the frequency ω' is a function of position within the resonance chamber. Therefore, a generalized form of Eq. (14) must be developed to relate the experimentally determined frequency of maximum absorption ω_c' to the true cyclotron frequency ω_c. If the difference between these two frequencies is denoted by

$$\delta\omega=\omega_c'-\omega_c, \tag{15}$$

Eq. (12) can be written in the form

$$\omega'=\omega_c'-\delta\omega-c\Gamma/2H. \tag{16}$$

If a normalized distribution function $\sigma(\Gamma)$ is introduced, where $\sigma(\Gamma)$ is that fraction of ions per unit Γ experiencing a field term Γ, Eqs. (12) and (14) yield

$$P(\omega-\omega_c')=\int_\Gamma \psi\left[\alpha\left(\omega-\omega_c'+\delta\omega+\frac{c\Gamma}{2H}\right)^2\right]\sigma(\Gamma)d\Gamma. \tag{17}$$

Two separate cases must now be discussed; that in

which the primary broadening mechanism is the ion lifetime distribution and that in which the broadening is due to the variation of Γ over the resonance chamber.

For the lifetime-broadened line, the linewidth parameter α is small enough (natural linewidth large enough) to prevent the resonance line shape from being controlled by $\sigma(\Gamma)$. Therefore, the value of $\delta\omega$ can be determined as α approaches zero. Differentiating both sides of Eq. (17) with respect to $(\omega-\omega_c')$ and setting $\omega=\omega_c'$ yields

$$\delta\omega=-\int_\Gamma \psi'\left[\alpha\left(\delta\omega+\frac{c\Gamma}{2H}\right)^2\right]\frac{c\Gamma}{2H}\sigma(\Gamma)d\Gamma \Big/ \int_\Gamma \psi'\left[\alpha\left(\delta\omega+\frac{c\Gamma}{2H}\right)^2\right]\sigma(\Gamma)d\Gamma, \quad (18)$$

where ψ' is the derivative of ψ with respect to $(\omega-\omega_c')$. Equation (18) yields:

$$\lim_{\alpha\to 0}\delta\omega=c\langle\Gamma\rangle/2H, \quad (19)$$

where

$$\langle\Gamma\rangle=\int_{\Gamma_{\min}}^{\Gamma_{\max}}\Gamma\sigma(\Gamma)d\Gamma.$$

Thus, for an electric-field-induced frequency shift $\delta\omega$ which is small compared to the resonance linewidth, Eqs. (15) and (19) combine to give

$$\omega_c'=\omega_c\left[1-\frac{Mc^2}{2eH^2}\langle\Gamma\rangle\right]. \quad (20)$$

Since ω_c' depends on the average value of Γ, and is not sensitive to the nature of the distribution function $\sigma(\Gamma)$, we conclude that the extrapolation procedure is valid.

For the case in which the primary resonance broadening is due to the variation in Γ over the chamber, the resonance line shape is determined largely by $\sigma(\Gamma)$ and need not be symmetric. In order to examine how the extrapolation procedure is to be applied we can write Eq. (17) in the form

$$P(\omega-\omega_c)=\int_\Gamma \psi\left[\alpha\left(\omega-\omega_c+\frac{c\Gamma}{2H}\right)^2\right]\sigma(\Gamma)d\Gamma. \quad (21)$$

Effects due to the distribution of Γ are now predominant over lifetime broadening so that α is large and ψ has the character of a δ function in Eq. (21). Therefore (21) becomes

$$P(\omega-\omega_c)\cong N\sigma(2H(\omega_c-\omega)/c), \quad (22)$$

where N is a normalization constant. We see that the line shape has the character of the distribution function σ and that it contracts linearly with increasing H.

Experimentally one determines a frequency $\omega=\omega_c'$ that is characteristic of the line; usually this is the point of maximum power absorption which occurs for some value, say A, of the argument in Eq. (22). Thus

$$(\omega_c-\omega_c')\times 2H/c=A,$$

or

$$\omega_c'=\omega_c\left[1-\frac{Mc^2}{2eH^2}A\right]. \quad (23)$$

This equation is identical to Eq. (20) in its dependence on H so that the extrapolation procedure is still valid.

It is possible to obtain a good indication of which broadening mechanism is predominant for a given run by examining the linewidth of the resonance as a function of magnetic field H. For the case of lifetime broadening the linewidth in cps depends only on some inverse mean lifetime and hence should be independent of H. For the electrostatic field broadened case the linewidth should be proportional to $1/H$ as indicated by Eq. (22). Most of the runs distinctly had one or the other of these dependences on H. Some runs, however, had a $1/H$ dependence of linewidth for small values of H and a constant value for large H. This indicates that there was a transition from electric field to lifetime broadening as H increased and the entire run must be rejected because the extrapolation procedure need not be valid under these conditions. It should be noted that such a transition should occur for *all* runs, were they carried over a sufficiently large range of H, because at very small values of H the electric field broadening must predominate as does the lifetime mechanism for large values of H. It is important to recognize, however, that the primary requirement for the validity of the extrapolation procedure in any run is that this transition does not occur within the magnetic field interval in which the data are taken.

The experiment has been designed to permit the investigation of ω_c'/ω_d over a magnetic field interval of 8000 to 12 500 gauss in which interval the cyclotron resonance varies from 6 to 10 Mc/sec. The measurements have been performed for a large variety of space charge and trapping conditions. The basic assumption of the extrapolation procedure, that Γ is independent of H, can be tested by examining the dependence of ω_c'/ω_d on $(1/H)^2$ for those runs where either lifetime *or* electric field broadening was clearly exhibited. We have found no systematic deviations from linearity for these runs and conclude that the extrapolation procedure is meaningful.

F. CYCLOTRON TUBE AND VACUUM SYSTEM

An enlarged view of the cyclotron tube is shown in Fig. 2. The tube is mounted directly above a glass vacuum seal. Molybdenum sheets of 0.01-in. thickness form the plates of the tube and are spot-welded to 0.03-in. diam tungsten rods that pass through the vacuum seal. The two grid plates (g_1 and g_2) and the screen have $\frac{1}{16}$-in. holes at their centers which are covered with fine tungsten grid mesh. The filament of

the tube is made from 0.004-in. tungsten wire wound in a helix. The helix has an inside diameter of 0.01 in. and is about $\frac{3}{8}$ in. long. The axis of the helix is vertical and hence perpendicular to the direction of the applied magnetic field and the rf electric field. The screen grid and the plate form the ends of the resonance chamber. The rf ground plate is shaped to form three sides of the chamber while the remaining rf plate is the fourth side.

Two separate tubes were used in this experiment. One tube had a chamber of dimensions $\frac{3}{4}\times\frac{3}{4}\times 1$ in., the other tube had a chamber which was almost cubic, the length of one side being $\frac{1}{2}$ in.

Figure 3 shows the assembled tube mounted at the end of the vacuum system. Directly above the tube is a liquid air trap of 1-liter capacity. The vacuum system consists of a roughing pump, an oil diffusion pump (G-25A), and a 3-liter liquid air trap. Mounted between the trap and the cyclotron tube is a leak made of thin-walled nickel tubing which, when heated, allows hydrogen to enter the vacuum system. A brass bellows is inserted between the pumps and the cyclotron tube so that the measurements can be performed without moving the vacuum system. Under typical operating conditions the vacuum obtainable by this system was 2×10^{-8} mm Hg as measured with a type VG-1A Consolidated vacuum gauge.

In order to obtain good cyclotron resonances it was necessary to bake the plates of the cyclotron tube at almost white heat which was achieved by rf induction heating with a Thermionic model-50 unit.

G. DEUTERIUM RESONANCE PROBE

The deuterium resonance probe was made from a Lucite block. The liquid chamber of the probe was of the same shape and dimensions as the cyclotron resonance chamber. Several turns of No. 28 copper wire were wound around the chamber to form the coil of an rf oscillator tank circuit. The Lucite block was mounted in a 1-in.-diam OFHC copper tube about 10 inches long which was situated as shown in Fig. 3. The top of the probe was covered with a thin-walled brass cap shown to be free of significant magnetic contamination.

H. INTERCHANGE MECHANISM

Although it would have been possible to perform the experiment with the cyclotron tube and the deuterium probe at separate points in the magnetic field this was not feasible because the extrapolation procedure required the measurement of ω_c'/ω_d over a wide range of magnetic fields. The magnetic field derivatives are field dependent and can be reproduced only by careful cycling.

Therefore, an interchange mechanism (Fig. 3) was developed so that the cyclotron and deuterium resonance frequencies could be measured at the same position in the magnetic field. To effect the interchange of the cyclotron tube and the deuterium probe a horizontal sliding aluminum table was employed. The cyclotron tube and deuterium probe were mounted on the table with the centers of their resonance chambers placed 2 in. apart. The sliding table is connected by a brass rod to an eccentric wheel mounted on the axis of a motor which is in turn mounted on the brass frame. Rotation of the wheel through 180° interchanged the position of the cyclotron tube and the deuterium probe. The interchange of the cyclotron tube and the deuterium probe was reproducible to within 0.05 in.

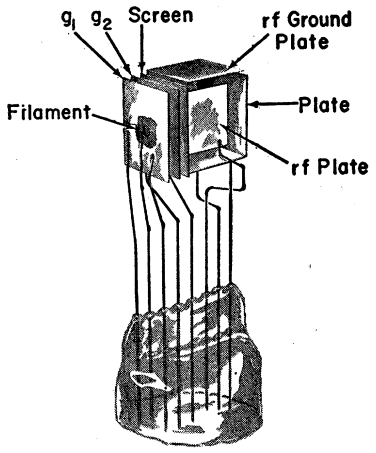

FIG. 2. Enlarged view of cyclotron tube.

I. ELECTRONICS[9]

A block diagram of the main electronic components is shown in Fig. 4.

The power supply for the cathode, grids, and plate of the cyclotron tube consisted of a battery box and a voltage control panel from which dc voltages were applied to the tube. The filament was powered by a

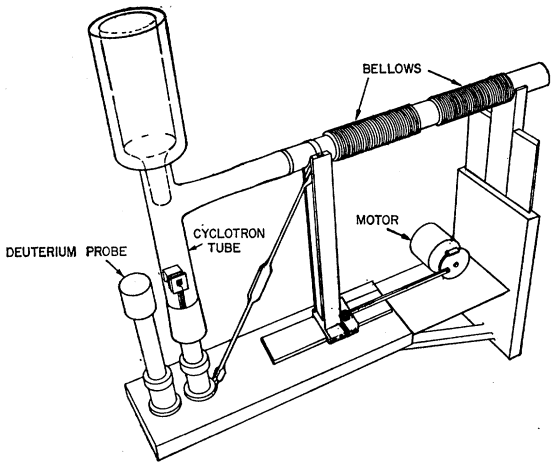

FIG. 3. Cyclotron tube and deuterium probe mounted on interchange mechanism. The apparatus to the left of the bellows can be moved back and forth by the motor. The nickel leak and other magnetic components are fixed to the right of the bellows and are not shown.

[9] Circuit diagrams are shown in reference 7.

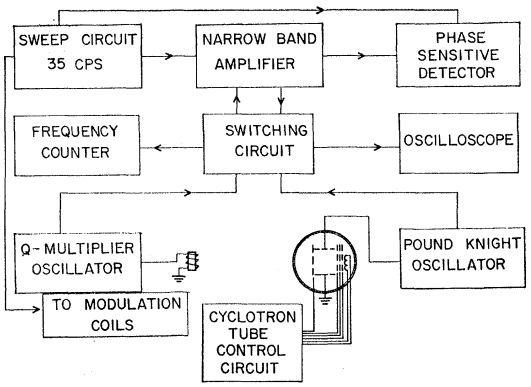

FIG. 4. Block diagram of cyclotron resonance apparatus.

20-kc/sec voltage source which was amplified through a Heathkit model A-9C audio amplifier. The plate current of the tube was regulated with a galvanometer-stabilizer circuit which controlled the filament temperature and provided a long-time current stability of $\sim 1\%$.

The rf plates of the cyclotron tube form part of the capacitance of a low-level sensitive regenerative oscillator similar in design to a Pound-Knight oscillator.[10] The rf oscillator voltage was amplified and detected, and the voltage level of oscillation was displayed on a Du Mont Laboratories type 304 oscilloscope.

Utilizing the calculations of the ion power absorption (Sec. B) together with an approximate model for the oscillator, the computed level of oscillation should diminish $\sim 10\%$ at the cyclotron resonance. The observed diminutions (signals) were usually of this order.

Typical broad-band signal to noise of the detected resonance was 3:1. This was improved by a factor of 100 with narrow-band techniques.

The magnetic field is modulated at 35 cps at an amplitude which is small compared to the resonance linewidth. The 35-cps component of the detected rf oscillator signal is then nearly proportional to the derivative of the power absorption curve and thus the point of maximum power absorption is indicated by a null in this signal.

The derivative of the resonance line shape can be traced upon a Varian Associates model G-10 recorder used in conjunction with the narrow-band amplifier and a phase sensitive detector.

A digital display of both the Pound-Knight oscillator frequency and the nuclear magnetic resonance frequency is obtained with a Hewlett-Packard model 524-B electronic counter.

The coil surrounding the deuterium sample is part of the tuned circuit of a sensitive regenerative oscillator discussed by Liebes and Franken.[6] The feedback is adjusted to obtain low-level oscillation. The oscillation is attenuated upon passage through resonance and the detected signal is fed into the narrow-band amplifier and displayed on the oscilloscope in the same manner as for the ion resonance.

J. MAGNETIC FIELD APPARATUS

A Varian Associates model V-4012 electromagnet and model V-2100 current regulator produces the magnetic field for this experiment. The pole faces of the magnet are 12 in. in diameter, separated by a 2-in. gap. Fields uniform to one part in 10^5 over a few cm^3 are obtained in the range of magnetic field from 8 to 12.5 kgauss. The most serious departure from homogeneity occurs in the magnetic field direction (see Fig. 10 and the discussion in Sec. N).

K. MEASUREMENT PROCEDURE

The procedure followed in the course of a typical run will now be outlined.

At the beginning of each series of runs the cyclotron tube was baked by induction heating for a period of ~ 30 min. The cyclotron tube and the deuterium probe were then placed in the magnetic field and the hydrogen leak was activated by running a constant current of ~ 5 amp through the nickel tube.

The cyclotron resonance was observed at some high field value and the cyclotron tube voltages and emission current were adjusted to give a symmetric resonance line. The symmetry of the line was determined by requiring equal amplitude of the narrow-band signal at the inflection points of the resonance curve. When the desired symmetry was obtained, the emission current regulator was activated.

The procedure in determining ω_c'/ω_d at a particular value of magnetic field (a "point") commenced with a measurement of cyclotron resonance frequency with the tube situated in the center of the magnet. The deuterium probe was then moved into the center and the deuterium resonance frequency was determined. This procedure was repeated with alternate measurements of both resonance frequencies. Usually five cyclotron frequency readings and four deuterium spin frequency readings were taken for one point in a period of about four minutes. It usually took five minutes to reset the magnetic field and adjust the frequencies for the next point. The emission current and the pressure of hydrogen in the vacuum system were monitored throughout each run.

The majority of the runs have been taken starting at a low value of magnetic field and increasing the field. Often at the end of a run the point corresponding to low magnetic field was repeated in order to check for systematic drift of either the emission current or space charge configuration. In several of the runs the points were taken in random order. No systematic shifts due to the order of data taking were detected.

L. EXPERIMENTAL RESULTS

Because of the z-axis magnetic field gradients (see Fig. 10 and the discussion in Sec. N), it was decided that

[10] R. V. Pound and W. D. Knight, Rev. Sci. Instr. **21**, 219 (1950).

TABLE I. Raw data and intercept values. Column B: dc cathode voltage of cyclotron tube. Column C: dc grid No. 1 voltage of cyclotron tube. Column D: dc grid No. 2 voltage of cyclotron tube. Column E: dc screen grid voltage of cyclotron tube. Column F: dc plate voltage of cyclotron tube. Column G: plate current of cyclotron tube. Column H: pressure of hydrogen in vacuum system. Column J: slope of straight line fit to data points on plot of ω_c/ω_d vs $1/H^2$. Column K: raw data straight line intercepts at $1/H^2=0$. Column L: deviation of intercept value from the mean intercept value. Column M: mean-square deviation of intercept value.

A	B	C	D	E	F	G	H	J	K	L	M
Run	V_c (v)	V_{G1} (v)	V_{G2} (v)	V_s (v)	V_p (v)	I_p (μa)	Pressure (10^{-6} mm Hg)	$\frac{\Delta(\omega_c/\omega_d)}{\Delta(1/\nu_d\times10^7)}$	ω_c/ω_d at $1/H^2=0$	$d(\omega_c/\omega_d)$	$d^2(\omega_c/\omega_d)$
1	−56	0	0	0.5	0.2	0.3	0.9	−195	1.165 969	12	144
2	−48	0	0	0.2	0.0	0.8	6.4	−131	1.165 957	0	0
3	−86	0	0	0.2	0.0	0.3	7.2	−136	1.165 944	−13	169
4	−80	22	22	0.2	0.0	0.4	6.2	−108	1.165 970	13	169
5	−70	0	22	0.2	0.0	0.3	4.3	−61	1.165 927	−30	900
6	−88	0	22	0.2	0.0	0.4	8.2	−98	1.165 955	−2	4
7	−86	0	0	0.2	0.0	0.7	4.6	−75	1.165 944	−13	169
8	−94	20	20	0.0	0.0	0.4	6.2	−84	1.165 950	−7	49
9	−94	0	0	0.0	0.0	0.4	7.0	−89	1.165 958	1	1
10	−92	0	20	0.0	0.0	0.4	5.4	−71	1.165 939	−18	324
11	−92	0	0	0.0	0.0	0.4	4.9	−69	1.165 972	15	225
12	−90	−78	0	0.0	0.0	0.6	4.4	−100	1.165 986	29	841
13	−90	0	0	0.1	0.0	0.3	6.3	−135	1.165 978	21	441
14	−90	0	0	0.0	0.0	0.3	4.2	−68	1.165 935	22	484
15	−90	0	0	0.0	0.0	0.3	2.6	−81	1.165 950	−7	49
16	−58	0	0	0.0	0.0	0.3	7.4	−54	1.165 931	−26	676
17	−90	0	0	0.0	0.2	0.6	4.4	−91	1.165 956	−1	1
18	−90	0	0	0.0	0.2	0.6	4.4	−156	1.165 975	18	324
19	−42	0	0	0.2	0.2	0.6	4.8	−141	1.165 965	8	64
20	−90	−88	0	0.0	0.0	0.9	4.0	−128	1.165 965	8	64
21	−40	0	0	0.0	0.1	0.9	3.7	−103	1.165 960	3	9
22	−40	0	0	0.0	0.1	1.8	2.6	−105	1.165 950	−7	49
23	−40	0	0	0.0	0.0	0.6	5.2	−93	1.165 966	9	81
24	−40	0	0	0.0	0.1	0.7	3.3	−91	1.165 955	−2	4

$\langle\omega_c/\omega_d\rangle_{av}=1.165\,957$
Variance of a single run: $s=15.1\times10^{-6}$
Standard deviation of the average: $S=s/\sqrt{N}=3.08\times10^{-6}$

only the data taken with the small resonance chamber would be included in the determination of μ_p/μ_n. However, it should be noted that the average value of the extrapolated intercepts ω_c/ω_d at $(1/H^2)=0$ for the small tube differed by only +4 ppm from that of the large tube. In addition, the deviations from the average value are somewhat less for the small resonance chamber.

A total of 29 runs were taken with the small tube. Of these, five have been rejected for reasons which will be discussed in Sec. M. Each of the runs contains from five to nine observations of ω_c'/ω_d at values of magnetic field ranging from 8000 to 12 500 gauss. (The graphs were actually plotted vs $1/\nu_d^2$, where ν_d is 6.5 Mc/sec at $H=10\,000$ gauss.) The extrapolated intercepts of ω_c'/ω_d at $(1/\nu_d^2)=0$ have been determined by fitting a least squares straight line to the raw data points of each of the 24 acceptable runs.

A summary of the operating conditions and of the results obtained for the 24 acceptable runs is contained in Table I in which column K contains the raw data extrapolated intercept values ω_c/ω_d of the least squares fitted straight lines. The average value is

$$\omega_c/\omega_d=1.165\,957, \tag{24}$$

and the standard deviation of the average is 3.1 ppm.

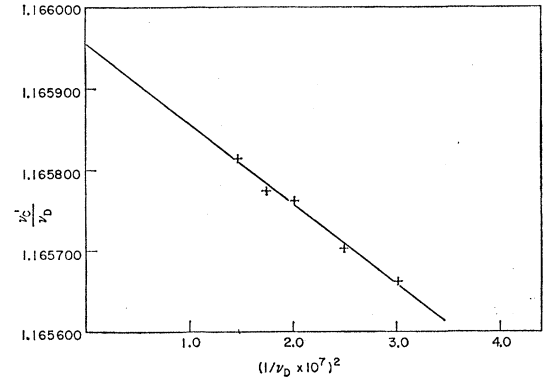

FIG. 5. Example of a poor run.

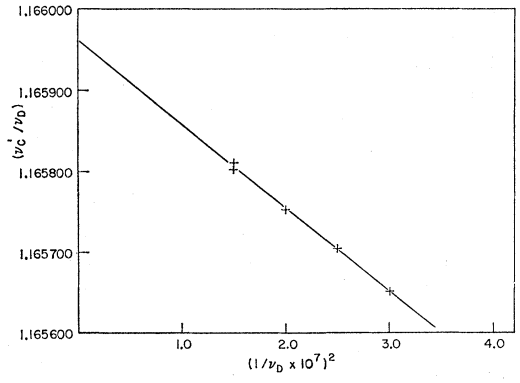

FIG. 6. Example of an average run.

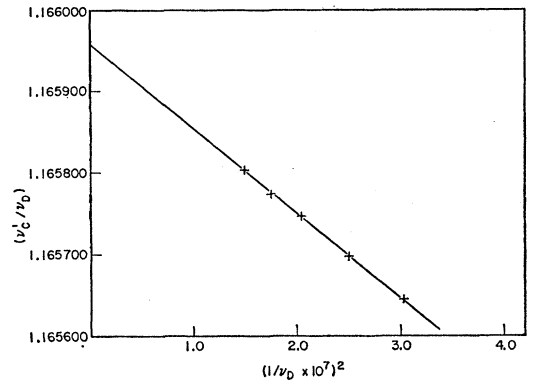

FIG. 7. Example of a good run.

Figures 5–7 show the details of poor, average, and good runs.

Figure 8 exhibits the straight lines obtained in each of the 24 accepted runs. The dashed line on this plot is that of one of the five rejected runs. This run did not clearly violate the acceptance conditions, but was rejected for reasons which will be discussed in Sec. M.

Figure 9 is a plot of the linewidth of the cyclotron resonance vs $1/\nu_d$ for extreme cases of lifetime and electrostatic broadening. Of the 24 accepted runs, the linewidths in thirteen were primarily due to electrostatic broadening and eleven were due primarily to lifetime broadening.

M. REJECTION OF RUNS

Four conditions had to be met for the acceptance of each run:

1. The pressure of hydrogen in the vacuum system had to be stable within 20% throughout the run.[11]
2. The emission current had to be constant within 1% throughout the run.
3. The width of the resonance line had to be either constant or linear in $1/H$ over the magnetic-field interval.
4. The symmetry of the resonance line had to be preserved throughout the run.

Conditions 1 and 2 were established to insure that the total space charge in the chamber was constant. Conditions 3 and 4 are related in that they partially determine the validity of the assumptions stated in Sec. E: (1) the electrostatic field term Γ is independent of the magnetic field, and (2) the electrostatic field distribution $\sigma(\Gamma)$ remains constant throughout the run.

Of the five rejected runs, one run violated conditions 1 and 2, two runs violated condition 3, and one run violated condition 4. The remaining rejected run is shown as a dashed line in Fig. 8. There is no clear basis for the rejection of this run under the conditions stated above and the plot is a straight line. The run is, however, rejected for the following reasons: (1) the extrapolated value of ω_c/ω_d at $(1/H^2)=0$ for this run lies far away from the remaining twenty-four runs; (2) the run has the same characteristic features as the run previously rejected on the basis of the fourth condition; and (3) the run is not reproducible. It is possible that, accidentally, some ferromagnetic material was situated so that it was systematically moved during this run. If this run is included with the remaining data, the average value of ω_c/ω_d is shifted by 2 ppm in such a direction as to increase the discrepancy between the results of this experiment and the currently accepted value.

If the extrapolated end points of the five rejected runs are included with those of the accepted runs, the average value of ω_c/ω_d is decreased by only 1 ppm.

[11] It was difficult to provide a pressure regulation consistently better than 20% throughout each run. In separate experiments, we have verified that the cyclotron resonance frequency does not shift significantly with variations in pressure of the order of 20%.

TABLE II. Sources of error.[12]

Source of error	Estimated 70% confidence interval
1. Error in estimating line-shape symmetry	± 6 ppm
2. Error due to magnetic field inhomogeneity	± 5 ppm
3. Possible deviations from linearity and the slope-intercept correlation effect	±18 ppm
Total 70% probable error $=[(6)^2+(5)^2+(18)^2]^{\frac{1}{2}}=\pm 20$ ppm	

[12] By 70% confidence interval is meant that interval in which we believe there is a probability of 0.7 that the true value lies. We have attempted to estimate an interval independently for each source of error and have compounded these as shown in Table II.

N. DISCUSSION OF ERRORS

The standard deviation for the average value of ω_c/ω_d is ± 3.1 ppm. We do not believe, however, that 3.1 ppm represents a realistic 70% probable error quotation for this experiment. It is our opinion that there are three major contributions to the total probable error which are summarized and compounded as shown in Table II.

These sources of error are discussed in the following sections.

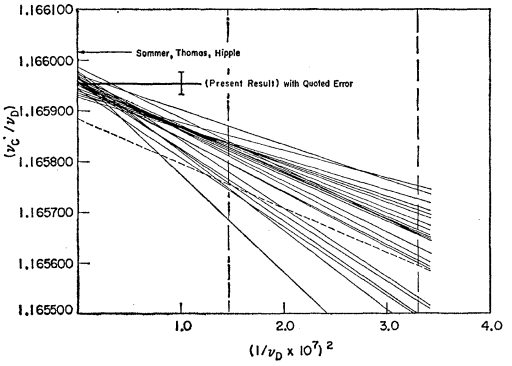

FIG. 8. Plots of the straight lines for each of the 24 runs.

1. Error in Estimating Line-Shape Symmetry

The experimental signal-to-noise ratios were such that the line symmetry could be estimated to the order of 1.5% of the linewidth. For typical operating conditions the half-width of the resonance line was 3.5 kc/sec at a resonance frequency of 7.5 Mc/sec so that the typical fractional linewidth $\Delta\nu/\nu$ was approximately 5×10^{-4}. Thus the symmetry of the line could be established to within ±7.5 ppm. Following careful consideration of the role of the line shape symmetry in this experiment we believe that a realistic 70% confidence interval to be associated with this effect is ±6 ppm.

2. Error due to Magnetic Field Inhomogeneity

It was found that in the space occupied by the resonance chamber the magnetic field inhomogeneity was much larger in a direction parallel to the magnetic field than in the perpendicular plane. Figure 10 exhibits a plot of the magnetic field as a function of distance from one pole face to the other for fields of 10 000 and 12 500 gauss. Measurements of this gradient were made with a small nuclear magnetic resonance probe. It is seen that the maximum disparity in the field is 30 ppm for the large chamber and 16 ppm for the small chamber.

This field gradient would have had no effect on the determination of ω_c/ω_d if both the cyclotron and the nuclear resonance frequencies corresponded to the same average magnetic field. Because of the short relaxation time of the deuterium sample it is known that the center of this resonance does correspond to the mean value of the magnetic field over the volume of the sample.[13] However, the distribution of the ions within the resonance chamber is not known so that the same correspondence cannot be demonstrated. For example, it is possible the major contribution to the cyclotron resonance absorption was due to ions clustered at the center or towards an edge of the chamber. Upon examination of Fig. 10 it can be seen that relative shifts in the ratio of effective magnetic field for the two resonances could

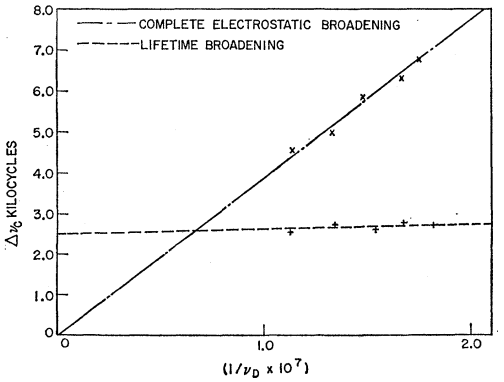

FIG. 9. Plot of two linewidths vs $1/H$.

[13] This averaging effect is the same as that discussed in Section E and is discussed in some detail in reference 6.

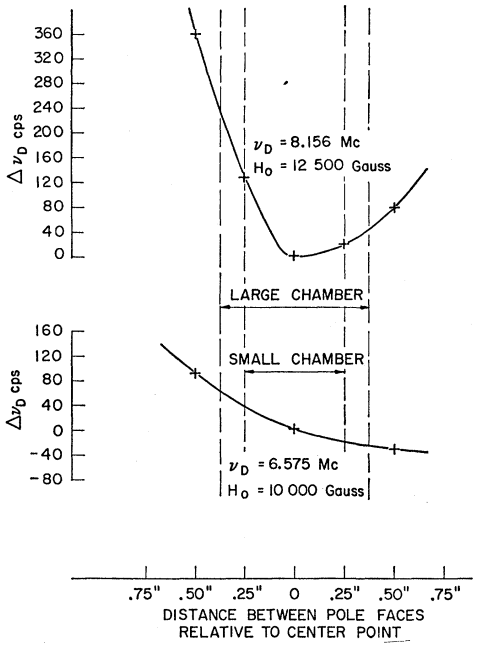

FIG. 10. Plot of magnetic field inhomogeneity.

be as large as 7 ppm, and of either sign. Therefore we apply no correction to the mean data of the experiment and we consider that ±5 ppm is a conservative estimate of the 70% confidence interval for this effect.

3. Possible Deviations from Linearity and the Slope-Intercept Correlation Effect

To test the validity of the straight line hypothesis, a composite line was constructed from all of the acceptable raw data in the following way. Adjacent data points on the plots of each of the 24 runs were connected by straight lines. Four equally spaced vertical line segments were then constructed on the graph of each run, and the intercepts of these vertical lines with the straight line segments were recorded. The points of Fig. 11 represent the average of these intercepts obtained at the position of each of the vertical lines on the individual graphs. The magnetic field values of the four points on the plot correspond closely to values at which the data were taken in each run.

The intercept at $(1/H^2)=0$ of a least squares adjusted straight line through the four points is

$$\omega_c/\omega_d=1.165\,956, \tag{25}$$

which agrees, to within 1 ppm, with Eq. (24).

The maximum deviation of any of the four points from this straight line is 1.4 ppm, and the mean deviation is 1.15 ppm. The points of the 24 runs used in making the composite have a mean deviation from their least squares straight lines of 6 ppm. If the straight line hypothesis is indeed valid, one would expect the mean deviation of the points of the composite to be $6/(23)^{\frac{1}{2}}$

$=1.25$ ppm, which is in very good agreement with the observed 1.15 ppm. Additional independent support for the straight line hypothesis is provided by comparing the 3-ppm standard deviation of the intercept in Fig. 11 with 3.1 ppm standard deviation of the average of the intercepts of the 24 separate runs.

Although the proper application of statistics to this experiment is limited, we believe that this analysis suggests very strongly that there were no large systematic deviations from straight line behavior. Furthermore, these statistics provide additional evidence that there were no random displacements of the separate lines caused, for example, by a varying magnetic contamination.

Unfortunately, the departure from a straight line does not have to be very large in order to seriously affect the value of the extrapolated point ω_c/ω_d at $1/H^2=0$. A confidence interval for the extrapolated end point can be obtained by examining the nonlinearity of the composite line.

To obtain some idea of the degree of nonlinearity of the composite line, a least squares adjusted quadratic function of the type

$$y=a+bx+cx^2, \tag{26}$$

where $y=\omega_c'/\omega_d$ and $x=1/\nu_d^2$, was fitted to the four points of Fig. 11 which determine the composite line. The values of a, b, and c are

$$a=1.165\,972,$$
$$b=-115.6\times10^{-6},$$
$$c=3.5\times10^{-6}.$$

The mean deviation of the points of Fig. 11 from this curve is 1.0 ppm, which is to be compared with the mean deviation of 1.15 ppm of the points from the straight-line fit.

The value of (a) is the extrapolated end point

$$\omega_c/\omega_d=1.165\,972, \tag{27}$$

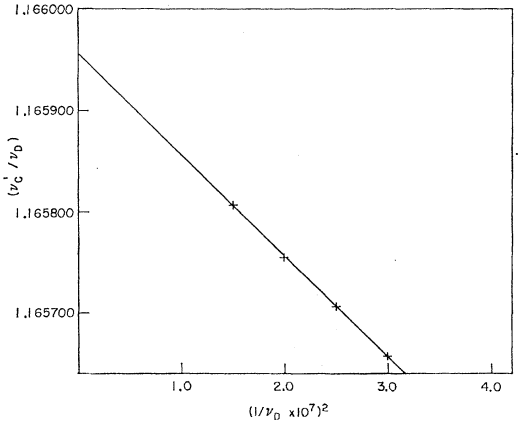

FIG. 11. Plot of composite line.

which is to be compared with Eq. (25). There is a 14-ppm discrepancy between the extrapolated end points of the straight line and the quadratic curve. However, if the two higher points of the composite line are moved by as much as one standard deviation (1.15 ppm) the discrepancy is in the opposite direction so that the quadratic curve cannot be regarded as particularly significant.

Of major concern to us is the apparent correlation between the intercept and the slope of each run,[14] which is exhibited in Fig. 12. Runs of shallow slope have lower intercept values than do those of steep slope. We believe that this effect may arise from the possibility that the electrostatic fields within the cyclotron resonance chamber are not constant over the magnetic field intervals of each run due to the field dependent drift of the ions within the chamber. (See Sec. E.) It is worth noting that this correlation effect is entirely absent in the work of Franken and Liebes[5,6] on the cyclotron resonance of free electrons in which experiment there was a firmer *a priori* justification of the independence of electrostatic fields with variation in magnetic fields.

We must therefore consider the possibility that the electrostatic field term Γ in Eq. (12) has a dependence on magnetic field. That is,

$$\Gamma=\Gamma_0+f(H), \tag{28}$$

where Γ_0 is independent of H, and $f(H)$ may depend upon the experimental conditions of each run. It is seen from Eq. (12) that the only way in which the field-dependent term $f(H)$ could contribute a large shift in the intercept without producing a concomitant curvature in the runs would be if this term were proportional to H^2.

In order to develop meaningful possibilities for the form of $f(H)$, two important constraints must be satisfied:

1. The models explored for investigation of the electrostatic field dependence on H must be physically meaningful.
2. The models must also predict results compatible with the rest of the data of the experiment, particularly those dealing with the linearity and the statistics of the runs discussed earlier in this section.

Since the electrostatic shifts in a typical run are much larger than the suspected error in this experiment we believe that the term $f(H)$ is small compared with Γ_0 so that a perturbation approach is justified. The perturbation is presumably due to a magnetic-field-dependent migration of the ions caused by mutually orthogonal components of electrostatic and magnetic field. The

[14] We would like to acknowledge the great benefit of many discussions one of us (P.A.F.) had with J. M. Sanders and J. C. Ward of the Clarendon Laboratories, Oxford, pertaining directly to this correlation effect as well as several other features of the present work and the experiment of Collington, Dellis, Sanders, and Turberfield.

instantaneous drift velocities in such circumstances are directly proportional to E and inversely proportional to H.

Since the charge distribution within the resonance chamber is not known we have considered many models that are compatible with the available information. For example, we can examine the effect of increasing magnetic field on cylindrical beams, on charge clouds that have dimensions very small compared with the chamber, diffuse clouds largely filling the chamber, etc. In these examinations we have performed expansions of $f(H)$ in direct and inverse powers of H and have found that the leading term in such expansions is always proportional to H or $1/H$. Terms proportional to H^2 also occur, of course, but these terms are smaller than the leading linear terms. Thus, in order to have significant effects due to H^2 terms there would have to be linear terms large enough to produce curvatures in the runs which are completely incompatible with the data of the experiment.

If leading terms in $f(H)$ proportional to H or $1/H$ are introduced in Eqs. (28) and (12), it is found that shifts in the extrapolated intercepts as large as 15 ppm can be produced without introducing curvatures in excess of 1.5 ppm in the magnetic field interval of this experiment. We believe that such terms may account for the apparent correlation shown in Fig. 12.

It is our opinion that the effects discussed in this subsection could not produce an error greater than 25 ppm without coming into striking conflict with the large body of experimental data. Since the shift can be of either sign, depending on the physical models, we make no correction to the data and we consider that ± 18 ppm is a realistic estimate of the 70% confidence interval for these effects.

4. Negligible Sources of Error

We have explored the errors that might be introduced by the variation in the hydrogen pressure during each run, the shifts that can occur due to magnetic contamination of the equipment, and the magnetic effect of the filament heater current.[7] We have concluded that the cumulative effect of these errors is less than 1 ppm and is therefore ignored in the estimation of the total error interval of this experiment.

O. REDUCTION OF $\omega_c(H_2^+)/\omega_d$ TO μ_p/μ_n

The ratio $\omega_c(H_2^+)/\omega_d$ is readily converted to $\mu_p(H_2O)/\mu_n$:

$$\frac{\omega_d}{\omega_c(H_2^+)}\frac{\omega_p(H_2O)}{\omega_d}\frac{M(H^+)}{M(H_2^+)}=\frac{\mu_p(H_2O)}{\mu_n}, \tag{29}$$

where $\omega_p(H_2O)/\omega_d$ is the measured ratio of the proton and deuteron spin resonance frequencies, $M(H^+)/M(H_2^+)$ is a very accurately known mass ratio, and $\mu_p(H_2O)/\mu_n$ is the magnetic moment of the proton (in water) in units of the nuclear magneton uncorrected for diamagnetic shielding.

The measurement of the ratio of the proton and deuteron spin resonance frequencies was performed at a constant magnetic field of 5000 gauss by interchanging the deuterium head employed in the measurement of ω_c/ω_d with a proton head. It will be recalled (Sec. G) that the deuterium sample was made cubic and was the same size as the cyclotron resonance chamber. The deuterium sample was D_2O doped with 0.33 molar $CuCl_2\cdot 2H_2O$. The proton sample was cylindrical with a length-to-diameter ratio of 1:1 and a volume nearly equal to the volume of the deuterium sample. The proton sample was H_2O doped with 0.01 molar $CuCl_2$, and was mounted in an OFHC copper tube of the same size and shape as the deuterium probe. Measurements were made by interchanging the position of the deuterium sample and the proton sample with respect to the center of the magnetic field. On the basis of 40 individual determinations of ω_p/ω_d, the ratio is

$$\omega_p/\omega_d=6.514\,411\pm 0.000\,003. \tag{30}$$

This ratio has been determined by Smaller[15] for undoped H_2O and D_2O:

$$\omega_p/\omega_d=6.514\,399\,8\pm 0.000\,002\,4. \tag{31}$$

The discrepancy between Smaller's result and the present measurement is 1.7 ppm and is almost certainly due to the paramagnetic Cu^{++} ions in our deuterium sample. The results quoted by Dickenson[16] for the shift

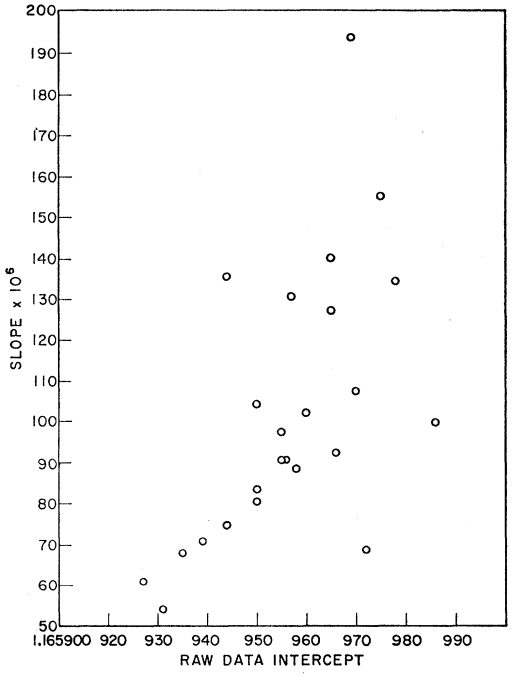

FIG. 12. Plot of slope vs intercept for each of the 24 accepted runs.

[15] B. Smaller, Phys. Rev. **83**, 812 (1952).
[16] W. C. Dickenson, Phys. Rev. **81**, 717 (1951).

in the magnetic field seen by the deuterons paramagnetic Cu^{++} ions indicates that the discrepancy is in the right direction and of the right order of magnitude. The effect of 0.01 molar $CuCl_2$ in the proton sample contributes a shift in the magnetic field seen by the protons of less than 3×10^{-8} according to the experimental results of Dickenson. Therefore, the ratio ω_p/ω_d will be referred to as the ratio for protons in pure water.

The mass ratio of the proton and the hydrogen molecular ion (neglecting dissociation energies) can be written as:

$$M(H_2^+)/M_p=2+(M_e/M_p).$$

Taking the ratio of the proton and electron mass as[17]

$$M_p/M_e=1836.12\pm0.02,$$

the mass ratio $M(H_2^+)/M_p$ becomes

$$M(H_2^+)/M_p=2.000\,544\,63,$$

and the reciprocal of this number is

$$M_p/M(H_2^+)=0.499\,863\,88, \qquad (32)$$

with an error of less than one part in 10^7. This error is negligible when compared with the error in the value of ω_c/ω_d.

From Eq. (24) and Table II, the value of ω_d/ω_c is

$$\omega_d/\omega_c=0.857\,665\pm0.000\,017. \qquad (33)$$

When the results (31), (32), and (33) are substituted into Eq. (29), the value obtained is

$$\mu_p(H_2O)/\mu_n=2.792\,83\pm0.000\,06, \qquad (34)$$

uncorrected for diamagnetic shielding.

H. Sommer, H. A. Thomas, and J. A. Hipple, reference 1.

To convert the observed value $\mu_p(H_2O)/\mu_n$ to $\mu_p(\text{free})/\mu_n$, we may write

$$\frac{\mu_p(\text{free})}{\mu_n}=\frac{\mu_p(H_2O)}{\mu_n}\,\frac{\omega_p(H_2)}{\omega_p(H_2O)}\,\frac{\omega_p(\text{free})}{\omega_p(H_2)}.$$

The combined correction for $\omega_p(\text{free})/\omega_p(H_2O)$[18,19] and $\omega_p(H_2)/\omega_p(H_2O)$[20,21] due to diamagnetic shielding is +26.1 ppm. When this correction is applied to Eq. (34),

$$\mu_p(\text{free})/\mu_n=2.792\,90\pm0.000\,06. \qquad (35)$$

P. REMARKS

The results of the four determinations of $\mu_p(H_2O)/\mu_n$ are listed below:

$\mu_p(H_2O)/\mu_n$		Method of determination of ω_c
2.792 68	0.000 06	Omegatron[1]
2.792 65	0.000 10	Inverse cyclotron[2]
2.792 68	0.000 05	Inverse cyclotron[3]
2.792 83	0.000 06	Present work

Our measurement and the average value of the other experiments is in disagreement by 50 ppm.

We believe that the principal liability of the present work arises from the uncertainty in the correlation and possible curvature effects discussed in Sec. N. In view of this we are currently modifying the apparatus to permit measurements up to 20 000 gauss. This will reduce the extrapolation range by a factor of three (see Fig. 8) so that these effects, if real, can be examined much more critically.

[18] N. F. Ramsey, Phys. Rev. **77**, 567 (1950); **78**, 699 (1950).
[19] G. F. Newell, Phys. Rev. **80**, 476 (1950).
[20] H. A. Thomas, Phys. Rev. **80**, 901 (1950).
[21] W. A. Hardy and E. M. Purcell (to be published).